

Supporting Information

Supporting Table S1. Templates for homology modeling

Model	DUSP1	DUSP7	DUSP13a	DUSP16	DUSP21	DUSP23b	DUSP28
Template	DUSP4	DUSP6	DUSP26	DUSP8	DUSP18	mouse DUSP23b	mouse DUSP28
Sequence identity	84.7%	87.5%	57.5%	73.0%	54.8%	80.0%	75.7%
Pdb code	3EZZ	1MKP	2E0T	This study	2ESB	3RGO	2HCM

Supporting Table S2. Optimal constructs for stable protein expression

Name	Residues	Residues in structure (PDB)	Active site mutation	Enzyme activity
DUSP1	173~323 (full:1~367) ¹	model	no	yes
DUSP2	172~312 (full:1~314)	170-314(1M3G)	yes ²	no
DUSP3	1~185 (full:1~185)	8-185(1VHR)	no	yes
DUSP4	174~338 (full:1~394)	193-336(3EZZ)	no	yes
DUSP5	178~321 (full:1~384)	174-320(2G6Z)	no	yes
DUSP6	205~350 (full:1~381)	204-347(1MKP)	no	yes
DUSP7	192~338 (full:1~368)	model	no	yes
DUSP8	159~312 (full:1~625)	160-310(this study)	no	yes
DUSP9	201~351 (full:1~384)	202-345(2HXP) 202-347(3LJ8)	no	yes
DUSP10	320~467 (full:1~482)	319-465(1ZZW) 315-482(2OUD)	no	yes
DUSP11	27~210 (full;1~330)	27-207(this study)	no	yes
DUSP12	27~191 (full:1~340)	27-189(this study)	no	yes
DUSP13a	1~188 (full:1~188)	model	no	yes
DUSP13b	1~198 (full:1~198)	25-193(2GWO) 25-192(2PQ5)	no	yes
DUSP14	1~198 (full:1~198)	24-191(2WGP)	no	yes
DUSP15	1~157 (full:1~243)	1-156(1YZ4)	no	yes
DUSP16	192~339 (full:1~665)	model	no	yes
DUSP17	Same as DUSP19	Same as DUSP19	yes	no

DUSP18	1~184 (full:1~188)	18-179(2ESB)	no	yes
DUSP19	65~206 (full:1~217)	65-206(3S4E)	yes	no
DUSP20	Same as DUSP18	Same as DUSP18	no	yes
DUSP21	21~183 (full:1~190)	model	yes	no
DUSP22	1~184 (full:1~184)	1-154(1WRM)	yes	no
DUSP23a	1~150 (full:1~150)	2-150(2IMG) 1-150(4ERC)	no	yes
DUSP23b	31~190 (full:1~201)	model	no	yes
DUSP24	Same as DUSP26	Same as DUSP26	no	yes
DUSP25	Same as DUSP23a	Same as DUSP23a	no	yes
DUSP26	61~211 (full:1~211)	60-211(4B04) 61-210(2E0T) 60-211(4HRF)	no	yes
DUSP27	2~220 (full:1~220)	32-206(2Y96)	no	yes
DUSP28	61~211 (full:1~211)	model	no	yes
PRL-1	4~163 (full:1~173)	-	no	yes
PRL-2	14~167 (full:1~167)	-	no	yes
SSH1	305~461 (full:1~1049)	-	no	yes
SSH2	305~449 (full:1~449)	-	no	yes
RNGTT	27~210 (full:1~545)	-	no	yes

¹, Residues numbers in parentheses represent those of full-length proteins. ; ², Because DUSPs 2, 19(17), 21, and 22 required the active site mutation (cysteine to serine) for stable protein expression, they were not used in the enzyme assay. Their expression constructs were listed in the table for possible usages in experiments other than enzyme assay. These usages may include structural studies, antibody generation, and protein interaction studies.

Supporting Table S3. Inhibition of enzyme activity by potential inhibitor compounds

	1	2	3	4	5	6	7	8	9	10
DUSP3 50nM	100.15	51.84	99.06	93.10	82.43	89.70	85.85	32.04	83.89	76.71
DUSP4 1 μ M	90.23	13.28	34.39	19.97	4.83	23.22	14.35	19.56	7.04	5.12
DUSP5 100nM	98.62	42.29	71.88	62.78	67.36	45.53	66.78	27.07	64.78	66.18
DUSP10 100nM	95.31	26.75	74.30	37.42	35.08	16.84	41.08	25.28	26.64	40.68
DUSP12 24 μ M	18.40	18.23	37.05	nd	nd	10.17	8.49	16.77	nd	nd
DUSP13a 500nM	100.27	4.22	60.72	20.05	0.32	20.79	8.61	nd	nd	nd
DUSP13b 2.5 μ M	78.45	23.58	33.78	30.10	25.78	20.08	55.78	25.04	29.41	8.71
DUSP15 100nM	99.46	35.69	91.38	53.19	47.12	47.69	53.29	28.55	54.40	60.03
DUSP16 6.7 μ M	47.73	21.00	31.59	17.57	8.32	15.67	26.30	23.47	10.92	3.80
DUSP18 11.8 μ M	95.62	32.33	47.38	26.51	20.43	47.79	39.10	28.85	14.49	10.61
DUSP23a 100nM	81.52	58.08	91.48	60.77	45.24	57.50	76.73	32.37	83.93	55.97
DUSP28 13.9 μ M	31.01	26.17	55.47	22.47	9.54	25.02	36.43	32.36	20.53	13.13
PRL1 10 μ M	21.22	29.10	52.94	25.67	17.16	24.25	19.15	42.70	16.72	12.18
PRL3 10 μ M	21.64	27.15	31.69	23.43	23.24	33.61	21.46	29.72	19.84	19.77
SSH1 100nM	100.31	19.83	73.14	36.17	31.10	15.90	44.92	17.06	32.18	43.99
SSH2 100nM	90.51	24.47	66.49	16.84	22.29	3.67	14.02	8.66	nd	8.03
RNGTT 16.7 μ M	57.76	32.99	36.15	17.82	17.70	7.46	18.03	25.72	14.11	12.04

DUSPs and related enzymes were treated with potential inhibitor compounds 1 to 10. Numbers in the table are percent inhibitions by respective inhibitor compounds. The percent inhibition values are the ratios of initial velocity of compound-inhibited enzyme reaction versus that of uninhibited (control) enzyme reaction. (see Materials and Methods). More than three measurements were averaged. Concentrations of enzymes used in the assay are indicated after the enzyme names (the left-most column). nd, not determined.

Supporting Table S4. Comparison of secondary structural elements

		$\alpha 0/\alpha 0'/\alpha 0''$ / $\beta 0$	$\alpha 1'/\alpha 1$	$\beta 4'/\alpha +$	$\alpha 5/\alpha 5'$	$\beta 6/\beta 7/\alpha 6$ / $\alpha 6'$
G1a	DUSP1	-	\sqrt{k}		$\alpha 5$	-
	DUSP4	-	\sqrt{k}	-	$\alpha 5$	-
	DUSP5	-	\sqrt{k}	-	$\alpha 5$	-
	DUSP8	-	\sqrt{k}	-	$\alpha 5$	-
	DUSP10	-	\sqrt{k}	$\alpha +$	$\alpha 5$	-
	DUSP16	-	\sqrt{k}		$\alpha 5$	-
G1b	DUSP2	-	$\alpha 1'+\alpha 1$ ^b	$\beta 4'$	$\alpha 5$	-
	DUSP6	-	$\alpha 1$	$\beta 4'$	$\alpha 5$	-
	DUSP7	-	$\alpha 1$	$\beta 4'$	$\alpha 5$	-
	DUSP9	-	$\alpha 1$	$\beta 4'$	$\alpha 5$	-
G2	DUSP15	-	\sqrt{k}	-	$\alpha 5^d$	-
	DUSP22	-	\sqrt{k}	-	$\alpha 5^d$	-
	DUSP12	-	\sqrt{k}	-	$\alpha 5$	$\alpha 6'^g$
	DUSP19	-	\sqrt{k}	-	$\alpha 5^e$	-
	DUSP28	-	\sqrt{k}	-	$\alpha 5$	-
G3	DUSP14	-	\sqrt{k}	-	$\alpha 5$	$\beta 6/\beta 7/\alpha 6$
	DUSP18	-	\sqrt{k}	-	$\alpha 5$	$\beta 6/\beta 7/\alpha 6$
	DUSP21	-	\sqrt{k}	-	$\alpha 5$	-
G4	DUSP3	$\alpha 0$	\sqrt{k}	$\alpha +$	$\alpha 5$	-
	DUSP13a	-	\sqrt{k}	$\alpha +$	$\alpha 5'$ ^f	-
	DUSP13b	$\alpha 0, \beta 0$	\sqrt{k}	$\alpha +$	$\alpha 5$	-
	DUSP26	-	\sqrt{k}	$\alpha +$	$\alpha 5'$	-
	DUSP27	$\alpha 0''^a$	\sqrt{k}	$\alpha +$	$\alpha 5$	-
G5	DUSP11	$\alpha 0'$	\sqrt{c}	$\alpha +$	$\alpha 5$	-
	DUSP23a	-	$\alpha 1$	$\alpha +$	$\alpha 5$	-
	DUSP23b	-	$\alpha 1$	$\alpha +$	$\alpha 5$	-

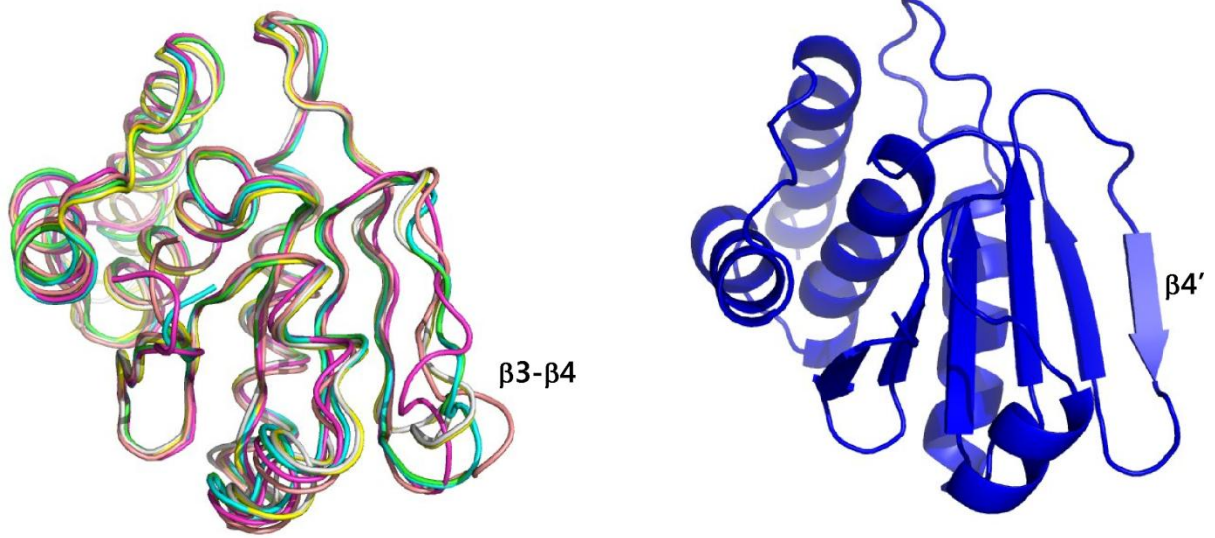
$\sqrt{\quad}$, presence of the secondary structural element; -, absence of the secondary structural element; $\alpha 1'+\alpha 1$, $\alpha 1'$ and $\alpha 1$ are connected to form a long helix; k, $\alpha 1$ and $\alpha 1'$ form a kinked helix; ^a, $\alpha 0''$ is located in the $\alpha 0$ position of the domain swapped dimer (bold); ^b, DUSP2 has $\alpha 1$ and $\alpha 1'$ connected together; ^c, DUSP11 has extended loops around $\alpha 1$ and $\alpha 1'$; ^d, the $\alpha 5$ s of DUSP15 and DUSP22 are longer than those of other DUSPs; ^e, the $\alpha 5$ of DUSP19 is divided into two helices; ^f, $\alpha 5'$ is located in the $\alpha 5$ position of the domain swapped dimer (bold); ^g, $\alpha 6'$ is located differently from $\alpha 6$.

Supporting Table S5. Extra cysteine residue and redox recovery efficiency

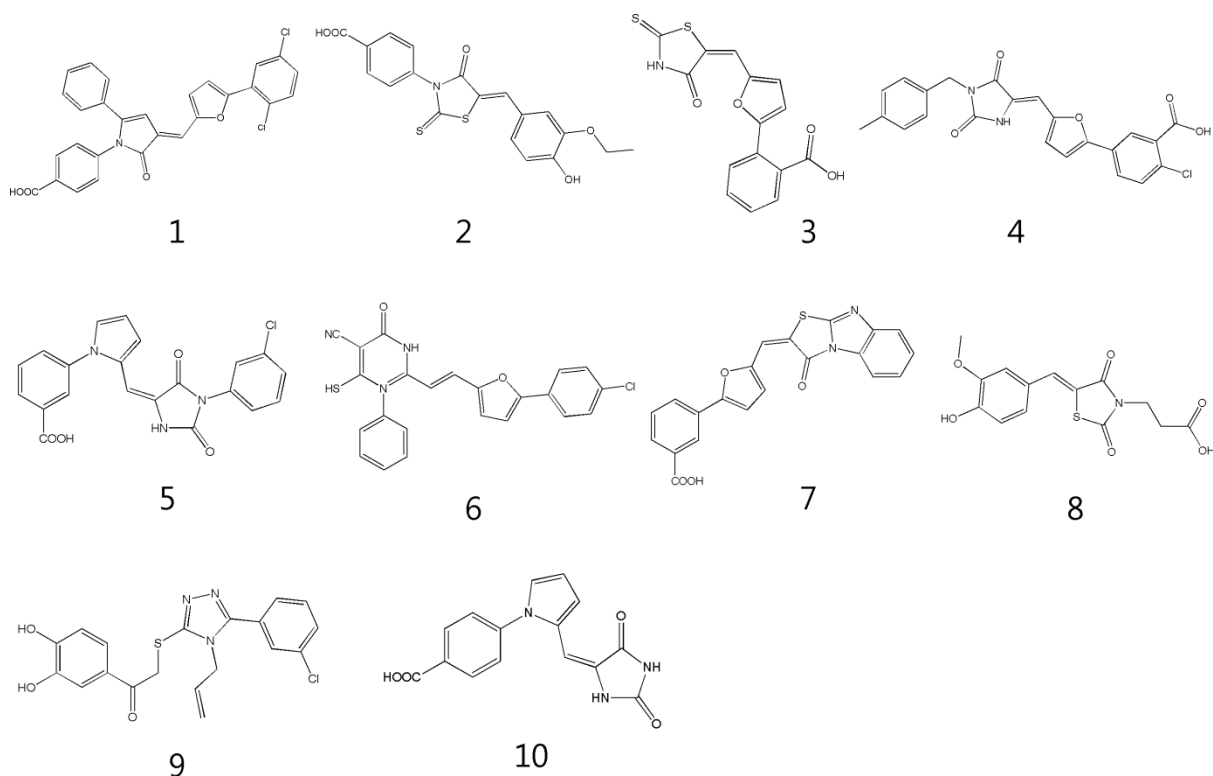
Name	Active cysteine	The closest cysteine	Inter-sulfur distance (Å) ^a	Recovery efficiency
DUSP1	Ser88	99	9.05	nd
DUSP2	Ser257	185	6.66	nd
DUSP3	Cys124	30	11.77	medium
DUSP4	Ser280	291	8.95	high
DUSP5	Ser263	274	8.56	medium
DUSP6	Ser293	218	9.03	nd
DUSP7	Cys90	15	10.58	nd
DUSP8	Ser246	197	6.61	nd
DUSP9	Cys90	84	22.07	nd
DUSP10	Cys408	400	23.41	medium
DUSP11	Ser152	164	12.13	nd
DUSP12	Ser115	97	12.55 ^b	medium
DUSP13a	Cys92	40	22.73	low
DUSP13b	Cys138	175	11.13	high
DUSP14	Cys111	122	8.72	nd
DUSP15	Ser88	70	10.97	low
DUSP16	Cys87	38	6.57	high
DUSP17	Same as DUSP19	-	-	-
DUSP18	Cys104	115	11.01	medium
DUSP19	Ser150	132	10.42	nd
DUSP20	Same as DUSP18	-	-	-
DUSP21	Cys84	95	11.41	nd
DUSP22	Cys88	124	8.62	nd
DUSP23a	Cys95	67	12.33	medium
DUSP23b	Cys95	44	11.32	nd
DUSP24	Same as DUSP26	-	-	-
DUSP25	Same as DUSP23a	-	-	-
DUSP26	Cys152	None	-	nd
DUSP27	Cys147	182	13.75	nd
DUSP28	Cys103	114	8.90	high

High, more than 70% recovery; medium, 30~70% recovery; low, less than 30% recovery; nd, not determined; ^a, For the proteins with the active cysteine to serine mutation, the distance between the OG atom of serine and the SG atom of the closest cysteine is listed in the table; ^b,

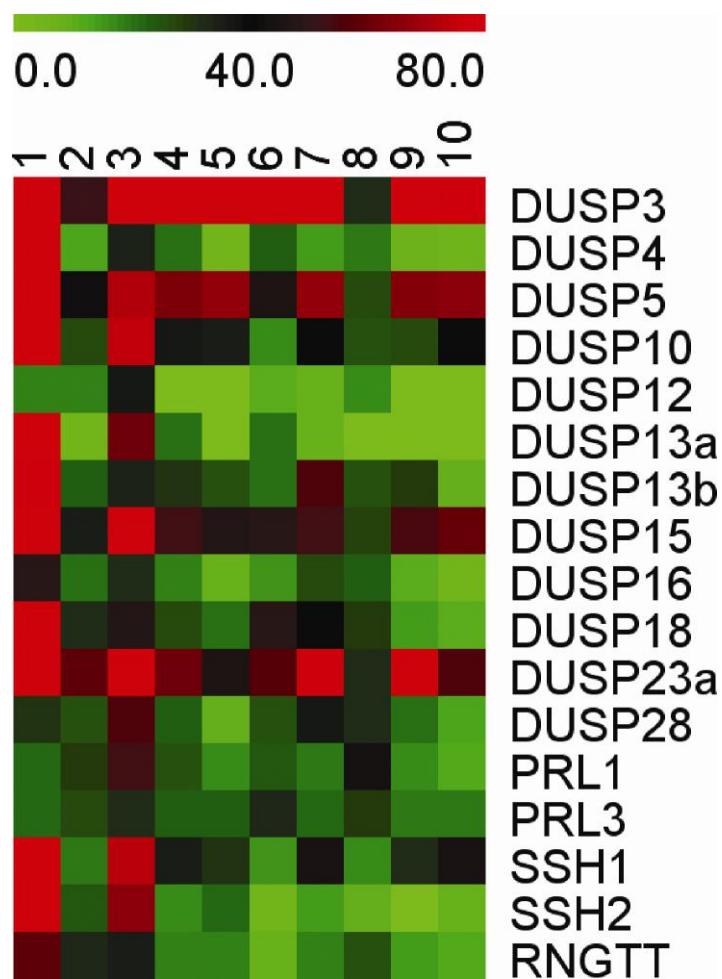
The CB atom of Ala97 is used for the distance calculation because Cys97 is mutated to alanine in crystallization. DUSPs with high recovery efficiency are indicated as grey.



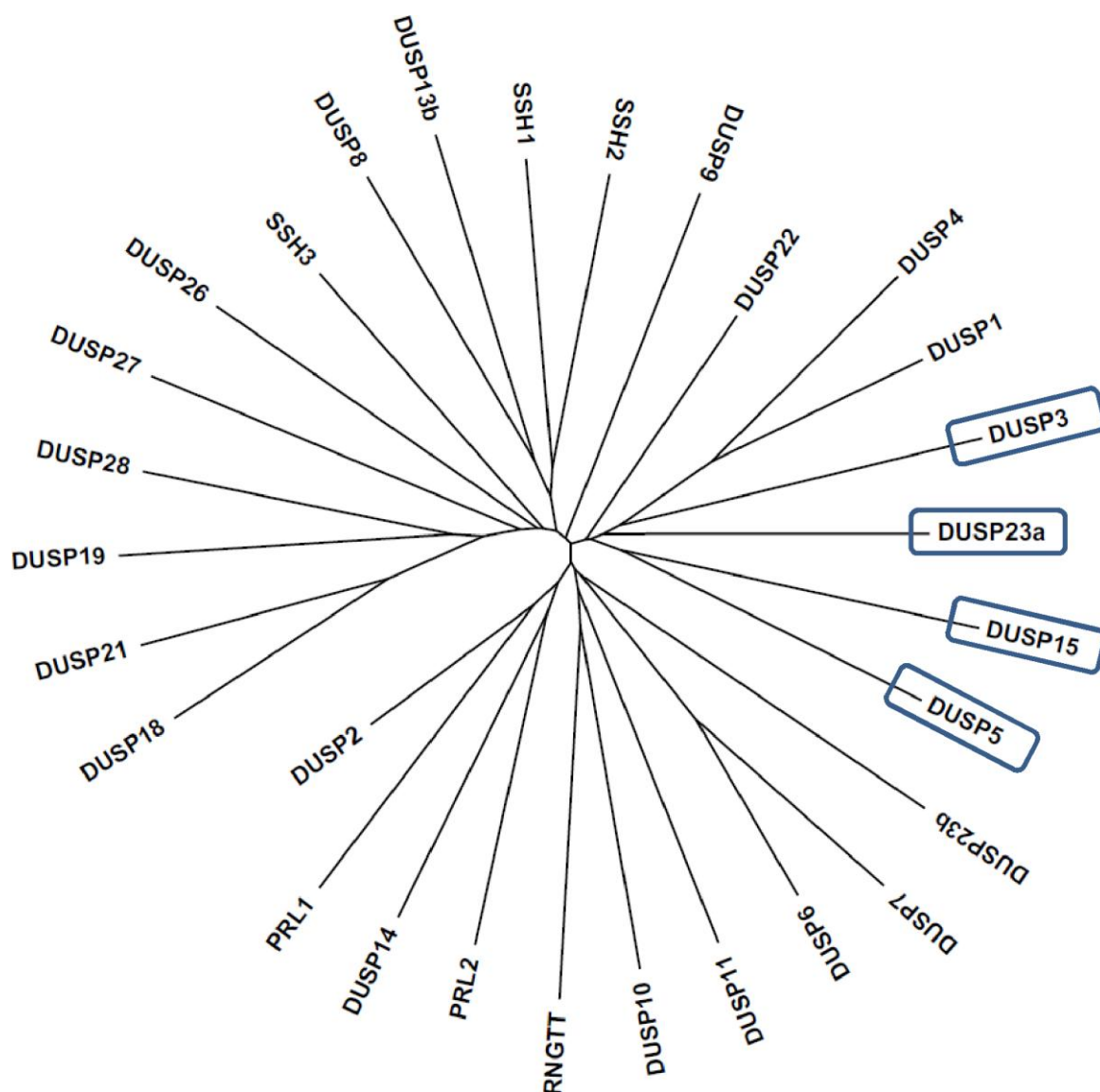
Supporting Figure S1. Variation of the $\beta3-\beta4$ loop conformation. Left: Structures of DUSPs 1, 4, 5, 8, 10, and 16 are superposed. In the figure, loop $\beta3-\beta4$ shows greater variability than other regions of the structure. Right: Ribbon diagram of DUSP9 shows the new strand $\beta4'$ created by the structural switch of loop $\beta3-\beta4$.



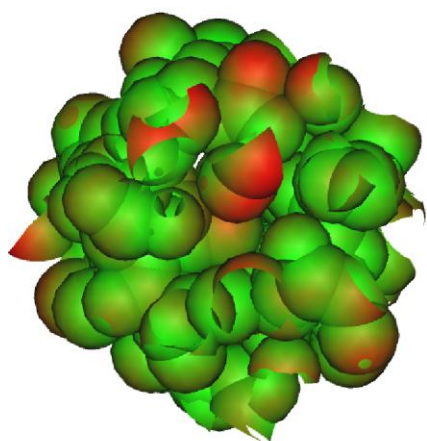
Supporting Figure S2. Chemical structures of inhibitor compounds. Chemical structures of previously identified inhibitor compounds are shown. Compounds 1, 2, 5, 6, 7, 9, and 10 are DUSP3 inhibitors (Park *et al.*, 2008b, Park *et al.*, 2010). Compounds 3, 4, 8, and 10 are DUSP1 inhibitors (Park *et al.*, 2011). Compounds 3, 5, and 6 are PRL-3 inhibitors (Park *et al.*, 2008a).



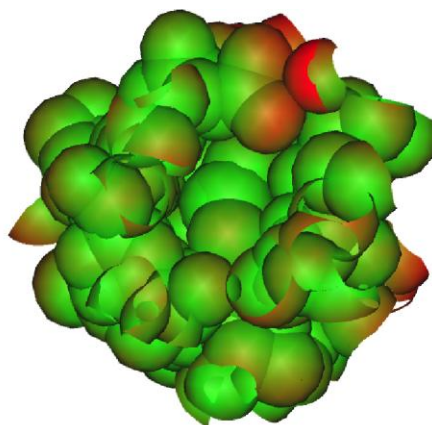
Supporting Figure S3. Inhibition profile. The results of DUSP inhibition assay in **Supporting Table S3** are presented as a color-coded diagram. In the figure, 0 (green) and 80 (red) represent no inhibition and 80% inhibition, respectively. The inhibitors 1-10 correspond to the compounds presented in **Supporting Figure S2**.



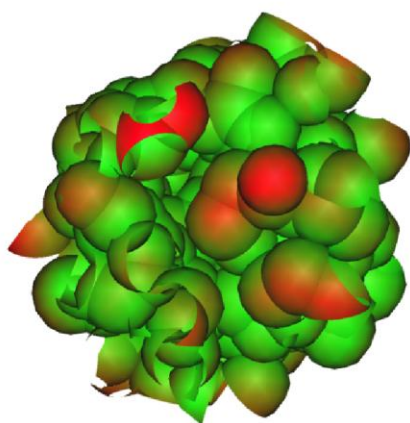
Supporting Figure S4. Phylogenetic tree of the active site surface geometry . The phylogenetic tree was constructed using similarity defined by the superposition of each pair of protein surfaces trimmed by the cutoff radius 6.0 \AA . $29 * 28/2 = 406$ superpositions were computed using the BetaSuperposer (Kim & Kim, 2012). The program MEGA (Tamura *et al.*, 2011) was used for phylogenetic tree construction. DUSPs having a similar inhibition profile (see text) are indicated as boxes.



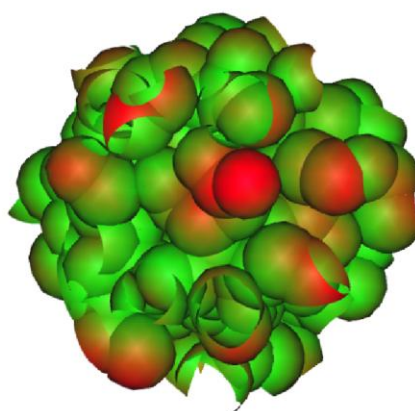
DUSP3/DUSP15



DUSP3/DUSP23a



DUSP3/DUSP13b



DUSP3/DUSP28

Supporting Figure S5. Active site pocket surface correlation. Active site pocket surface correlations between DUSP3 and different DUSPs were estimated by the voronoid calculation and the RMS deviations between beta points were displayed as color grading. The figures are shown at an equivalent orientation with the active site cysteine in the center. More red color represents beta-points with more deviation while more green color does those with less deviation. RMS deviations for DUSPs 15, 23a, 13b and 28 are 1.288, 1.091, 1.369, and 1.460 Å, respectively.

Supporting References

Kim, J. K. & Kim, D. S. (2012). *J. Biomol. Struct. Dyn.* **30**, 684-700.

Park, H., Jeon, J. Y., Jeong, D. G. & Ryu, S. E. (2010). *Bull. Korean Chem. Soc.* **31**, 3785-3787.

Park, H., Jeon, J. Y., Kim, S. Y., Jeong, D. G. & Ryu, S. E. (2011). *J. Comput. Aided. Mol. Des.* **25**, 469-475.

Park, H., Jung, S. K., Jeong, D. G., Ryu, S. E. & Kim, S. J. (2008a). *Bioorg. Med. Chem. Lett.* **18**, 2250-2255.

Park, H., Jung, S. K., Jeong, D. G., Ryu, S. E. & Kim, S. J. (2008b). *ChemMedChem*, **3**, 877-880.

Tamura, K., Peterson, D., Peterson, N., Stecher, G., Nei, M. & Kumar, S. (2011). *Mol. Biol. Evol.* **28**, 2731-2739.